Conformational Analysis of a Highly Potent Dicyclic Gonadotropin-Releasing Hormone Antagonist by Nuclear Magnetic Resonance and Molecular Dynamics

Rachelle J. Bienstock,† Josep Rizo,† Steven C. Koerber,‡ Jean E. Rivier,‡ Arnold T. Hagler,§ and Lila M. Gierasch†

Department of Pharmacology, University of Texas Southwestern Medical Center, 5323 Harry Hines Boulevard, Dallas, Texas 75235-9041, The Clayton Foundation Laboratories for Peptide Biology, The Salk Institute, 10010 North Torrey Pines Road, La Jolla, California 92037, and Biosym Technologies, Inc., 9685 Scranton Road, San Diego, California 92121

Received May 12, 1993•

Structural analysis of constrained (monocyclic) analogues of gonadotropin-releasing hormone (GnRH) has led to the development of a model for the receptor-bound conformation of GnRH and to the design of highly potent, dicyclic GnRH antagonists. This is one of the first cases where a dicyclic backbone has been introduced into analogues of a linear peptide hormone with retention of high biological activity. Here we present a conformational analysis of dicyclo(4-10,5-8)[Ac-D-2Nal[1]-D-*p*ClPhe[2]-D-Trp[3]-Asp[4]-Glu[5]-D-Arg[6]-Leu[7]-Lys[8]-Pro[9]-Dpr[10]]-NH_2 (**I**), using two-dimensional nuclear magnetic resonance (NMR) spectroscopy and molecular dynamics simulation. Compound **I** inhibits ovulation in the rat at a dose of 5–10 μg (Rivier et al. In *Peptides: Chemistry, Structure ad Biology*; Rivier, J. E., Marshall, G. R., Eds.; ESCOM: Leiden, The Netherlands, 1990; pp 33–37). The backbone conformation of the 4–10 cycle in this dicyclic compound is very similar to that found previously for a parent monocyclic (4–10) GnRH antagonist (Rizo et al. *J. Am. Chem. Soc.* **1992**, *114*, 2852–2859; *ibid.* 2860–2871), which gives strong support to the hypothesis that GnRH adopts a similar conformation upon binding to its receptor. In this conformation, residues 5–8 form a "β-hairpin-like" structure that includes two transannular hydrogen bonds and a Type II′ β turn around residues D-Arg[6]-Leu[7]. The "tail" of the molecule formed by residues 1–3 is somewhat structured but does not populate a single major conformation. However, the orientation of the tail on the same side of the 4–10 cycle as the 5–8 bridge favors interactions between this bridge and the tail residues. These observations correlate with results obtained previously for the parent monocyclic (4–10) antagonist, and have led to the design of a series of new dicyclic GnRH antagonists with bridges between the tail residues and residues 5 or 8.

Gonadotropin-releasing hormone (GnRH), *p*Glu[1]-His[2]-Trp[3]-Ser[4]-Tyr[5]-Gly[6]-Leu[7]-Arg[8]-Pro[9]-Gly[10]-NH_2, is secreted by the hypothalamus and stimulates the pituitary to produce luteinizing hormone and follicle stimulating hormone. Intense research has been dedicated to the development of GnRH analogues which could potentially be used as nonsteroidal contraceptive agents and for treatment of sex steroid dependent pathologies.[1] The design of GnRH analogues is hindered by the lack of direct information on the active conformation of the native hormone, as the tertiary structure of the GnRH receptor is unknown and GnRH itself is unstructured in solution.[2] This is a very common situation in drug design based on peptide hormones and neurotransmitters. The strategy that is emerging as the most effective to overcome these problems is based on the introduction of covalent constraints to force or stabilize particular structural features.[3] Structural analysis of the constrained analogues can help define the corresponding active conformation and suggest ways to obtain more potent analogs, which ultimately can lead to peptidomimetics with the desired activity. As described below, application of this approach to the design of GnRH antagonists[3d,4,5] has allowed us to obtain highly potent, dicyclic GnRH analogues.[6] These compounds are among the most constrained analogues of a linear peptide hormone that have ever been synthesized, with retention of high biological activity.

Analysis by nuclear magnetic resonance (NMR) spectroscopy and molecular dynamics simulation, combined with synthetic optimization of the bridges that bring about the constraints, have played a major role in the design of dicyclic GnRH antagonists. Early molecular dynamics studies[7] indicated that native GnRH can adopt conformations close to those adopted by a designed cyclic decapeptide antagonist, cyclo(Δ[3]-Pro[1]-D-*p*ClPhe[2]-Trp[3]-Ser[4]-Tyr[5]-D-Trp[6]-NMeLeu[7]-Arg[8]-Pro[9]-βAla[10]). This marginally potent GnRH antagonist was studied by molecular dynamics simulation[8] and by NMR spectroscopy[9] and found to adopt a remarkably rigid structure. It was hypothesized that some mobility in the termini was necessary to increase biological activity, and bridged 4–9 and 4–10 analogues were designed based on the proximity of residues Ser[4] and Pro[9] observed in low-energy conformations of this cyclic decapeptide antagonist.[3d] The 4–10 cyclization resulted in very potent GnRH antagonists, with activity comparable to that of the most potent linear analogues.[4] A detailed conformational analysis of one of these cyclo(4–10) GnRH antagonists, Ac-Δ[3]-Pro[1]-D-*p*F-Phe[2]-D-Trp[3]-cyclo(Asp[4]-Tyr[5]-D-2Nal[6]-Leu[7]-Arg[8]-Pro[9]-Dpr[10])NH_2 (which we refer to as the Asp[4]-Dpr[10] analogue), revealed that interactions between the side chains of residues 5 and 8, and between these side chains and the tail formed by residues 1–3, were likely to exist, suggesting new bridging opportunities for more constrained GnRH antagonists.[5] The first series of dicyclic GnRH analogues that we have synthesized contains 4–10 and 5–8 bridges,

† University of Texas Southwestern Medical Center.
‡ The Salk Institute.
§ Biosym Technologies, Inc.
• Abstract published in *Advance ACS Abstracts*, September 15, 1993.

0022-2623/93/1836-3265$04.00/0

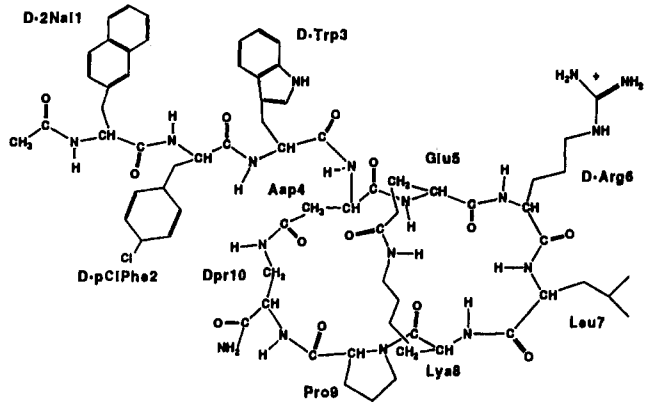

Figure 1. Schematic representation of the dicyclic GnRH analogue. The nomenclature and abbreviations used to designate amino acid residues throughout the text follow the recommendations of the IUPAC-IUB Commission on Biochemical Nomenclature (*Biochemistry* **1970**, *9*, 3471-3479). Other abbreviations used are as follows: 2Nal or Na, 3-(2'-naphthyl)alanine; *p*ClPhe or F, 4-chlorophenylalanine; Dpr or Dp, 2,3-diaminopropionic acid. The nomenclature used to designate the aromatic ring positions in D-2Nal[1] is as described in ref 5.

and some of these compounds display potencies equal to that of the corresponding monocyclic (4–10) antagonists (Table I).[6]

We have selected one of the most potent dicyclic GnRH antagonists, dicyclo(4–10,5–8)[Ac-D-2Nal[1]-D-*p*ClPhe[2]-D-Trp[3]-Asp[4]-Glu[5]-D-Arg[6]-Leu[7]-Lys[8]-Pro[9]-Dpr[10]]-NH_2 for structural analysis by NMR spectroscopy and molecular dynamics simulation. This GnRH antagonist, which we will refer to as the dicyclic analogue, is shown schematically in Figure 1. Our data indicate that residues 5–8 adopt a β-hairpin conformation that includes a Type II' β turn around residues 6–7. The tail (residues 1–3) is oriented above the ring (residues 4–10) and may be interacting with the Glu[5]-Lys[8] bridge. This structural model is very similar to that observed for the parent Asp[4]-Dpr[10] analogue.[5] The observation that the conformation of the 4–10 ring is retained upon introduction of an additional constraint and elimination of two potentially interactive side chains gives strong support to the hypothesis that a similar backbone conformation is adopted by GnRH when bound to its receptor.

Experimental Procedures

Peptide Synthesis. Instruments. Amino acid analyses (after 4 M methanesulfonic acid hydrolysis at 100 °C for 24 h) were performed on a Perkin-Elmer (Norwalk, CT) high-pressure liquid chromatograph using *o*-phthalaldehyde postcolumn derivatization and fluorescence detection. Preparative HPLC was run using a Waters Assoc. (Milford, MA) Prep LC/System 500A and a Model 450 variable-wavelength UV detector, a Fischer (Lexington, MA) Recordall Model 5000 strip-chart recorder, and a Waters Prep LC 500A preparative gradient generator. Analytical HPLC was run on a system using two Waters M-45 pumps, a Shimadzu Chromatopac EIA integrator, and a rheodyne Model 7125 injector. The peptide synthesizer used was a Beckman Model 990. Optical rotation was determined with a Perkin-Elmer Model 241 polarimeter. LSIMS mass spectra were measured using a Jeol JMS-HX110 double focusing mass spectrometer (Jeol, Tokyo, Japan) fitted with a Cs^+ gun. An accelerating voltage of 10 kV and Cs^+ gun voltage of 25 kV were employed. The sample was added directly to a glycerol and a 3-nitrobenzyl alcohol (1:1) matrix.

Starting Materials. Amino acid derivatives Boc-D-Trp, Boc-Asp(chx), Boc-Glu(OFm), Boc-D-Arg(Tos), Boc-Leu, Boc-Lys-(Fmoc), and Boc-Pro were obtained from Bachem Inc. (Torrance, CA). Boc-D-2Nal, Boc-D-*p*ClPhe, and Boc-Dpr(Z) were synthesized at the Southwest Foundation for Biomedical Research (under contract NO-1-HD-6-2928 with (NIH) and made available by the Contraceptive Development Branch, Center for Population Research, NICHD. The methylbenzhydrylamine resin (MBHAR) used for peptide synthesis was obtained according to published procedures.[10]

Peptide Synthesis. Peptides were prepared by solid-phase peptide synthesis methodology on a Beckman 990 peptide synthesizer using the Boc strategy, with synthetic protocols, including HF treatment as previously described.[4]

Cyclo(5–8)[Ac-D-2Nal[1]-D-*p*ClPhe[2]-D-Trp[3]-Asp[4](NHNH$_2$)-Glu[5]-D-Arg[6]-Lys[8]Dpr[10]]GnRH. Ac-D-2Nal-D-*p*ClPhe-D-Trp-Asp(chx)-Glu(OFm)-D-Arg(Tos)-Leu-Lys(Fmoc)-Pro-Dpr(Z)-MBHAR (4 g 0.45 nmol/g substitution) was deprotected of the Fmoc and OFm groups with 20% piperidine in DMF (2 × 15 min) and then washed with DMF, MeOH, 10% TEA/CH_2Cl_2, and CH_2Cl_2 (2 × 1 min each). The 5/8 side chain amide bond was formed on the resin using repeated BOP couplings as described by Felix et al.[11] and following the cyclization until the ninhydrin test was negative. The resin–peptide was sequentially washed with DMF (2 × 1 min), MeOH (2 × 1 min), and CH_2Cl_2 (2 × 1 min) and vacuum dried overnight. The decapeptide–resin was treated with anhydrous hydrazine (10 mL) in DMF (10 mL) and stirred 72 h at 23 °C. The peptide resin was collected by filtration and washed with DMF, MeOH, and CH_2Cl_2 (2 × 1 min) each. After vacuum drying, the peptide was cleaved from the resin by treatment with anhydrous HF (100 mL) and anisole (6 mL) for 40 min at 0 °C. The HF and anisole were removed by distillation under high vacuum. The remaining solid was washed with Et_2O (2 × 100 mL) and filtered. Extraction of the peptide with CH_3CN/H_2O (1/2) (2 × 100 mL) followed by lyophilization gave a fluffy white powder (1.1 g).

Cyclo(4–10/5–8)[Ac-D-2Nal[1]-D-*p*ClPhe[2]-D-Trp[3]-Asp[4]-Glu[5]-D-Arg[6]-Lys[8]-Dpr[10]]GnRH. The decapeptide (1 g, 0.7 mmol) was dissolved in 18 mL of DMF and held at −25 °C while 4 N HCl in dioxane (0.85 mL, 35 mmol) was added followed by isoamyl nitrite in three aliquots (0.5 mL, 1 mmol total) over 15 min. After 1 h at −25 °C the reaction mixture was diluted with previously chilled DMF (−25 °C) to 1 L. Diisopropylethylamine was then added to adjust the pH between 7 and 8 (moist pH paper, range 7–8). After 3 days at −15 °C the solvent was removed under vacuum and the yellow oil dissolved in CH_3CN/H_2O (100 mL) and lyophilized to yield the crude preparation of the dicyclic peptide (1 g, 0.7 mmol).

Purification. The lyophilized, crude peptide was dissolved in 0.25 M triethylammonium phosphate (200 mL), pH 2.25 (TEAP 2.25), and loaded onto a 5 × 30-cm preparative reversed-phase HPLC cartridge packed in our laboratory using Vydac C_{18} silica (330-Å pore size, 15–20-μm particle size). The peptide was eluted at a flow rate of 100 mL/min on a Waters Prep 500 System with a mixture of A (TEAP 2.25) and B (60% CH_3CN, 40% A) with an appropriate gradient (90 min) such that retention time was ~45 min. The collected fractions were screened by use of analytical reversed-phase HPLC under isocratic conditions, 0.1% TFA/H_2O at a flow rate of 2.0 mL/min (Vydac C_{18} column, 5 μm, 300 Å pore size, 4.5 × 250 mm). Appropriate fractions were then combined and converted to the TFA salt by loading after dilution (1/1) in water on a preparative reversed-phase HPLC cartridge as described above and eluted with the use of a mixture of solvents A (0.1% TFA) and B (60% CH_3CN, 40% A) and the following gradient: 20% B (10 min) followed by a 40-min gradient to 90% B. Selected fractions were pooled and lyophilized to yield 155 mg of the dicyclic peptide of high purity: HPLC (t_R = 4.7 min), eluent CH_3CN–0.1% TFA (34.8:65.2); FAB-MS (M^+) calculated 1412.59, found 1412.66. Amino acid analysis 2Nal 1.20, *p*ClPhe 1.11, Trp 0.80, Asp 0.90, Glu 1.05, Arg 1.00, Leu 0.93, Lys 1.00, Pro 0.92, Dpr was not determined. $[\alpha]_D$ = −52° (c = 0.64, 50% AcOH).

Nuclear Magnetic Resonance. Most NMR experiments were performed on a sample prepared by dissolving 5.1 mg of the dicyclic analogue in 0.340 mL of 99.96 atom % D DMSO-d_6 and 0.460 mL of 99.96 atom % D $CDCl_3$ (Sigma). The residual DMSO resonance at 2.49 ppm was used as an internal reference. The conformation of the dicyclic analogue was also studied in a hydrophilic solvent system by dissolving 3.42 mg of peptide in

Table I. Biological Potency of Constrained GnRH Antagonists in the Antiovulatory Assay

	compd	AOA[a]
cyclic decapeptide	cyclo(1-10)[Δ^3Pro^1-D-*p*ClPhe^2-D-Trp^3-D-Trp^6-NMeLeu^7-β-Ala^{10}]GnRH	1000 (5/8)[b]
Asp^4-Dpr^{10} analogue	cyclo(4-10)[Ac-Δ^3Pro^1-D-*p*FPhe^2-D-Trp^3-Asp^4-D-2Nal^6-Dpr^{10}]GnRH	10 (2/10)[c]
dicyclic analogue	dicyclo(4-10,5-8)[Ac-D-2Nal^1-D-*p*ClPhe^2-D-Trp^3-Asp^4-Glu^5-D-Arg^6-Lys^8-Dpr^{10}]GnRH	5 (2/10)[c]

[a] AOA-antiovulatory assay in the rat: dosage in μg (rats ovulating/total rats). [b] Reference 3b. [c] Reference 6.

0.200 mL of 99.94% deuterated trifluoroethanol (TFE-d_3) (Cambridge Isotopes) and 0.600 mL of water adjusted to pH 4.0.

All NMR spectra were acquired on a 500-MHz (proton frequency) Varian VXR 500 spectrometer. Sequential resonance assignments were obtained using 2D total correlation spectroscopy (TOCSY),[12] 2D-correlated spectroscopy (COSY),[13] and 2D nuclear Overhauser spectroscopy (NOESY)[14] experiments. One-dimensional spectra and 2D J-resolved spectra[15] were used to measure $J_{HN\alpha}$ and $J_{\alpha\beta}$ coupling constants. The methods and parameters used for data acquisition and processing are analogous to those used previously for the Asp^4-Dpr^{10} analogue.[5] In experiments carried out in H_2O/TFE-d_3 (3:1, v/v), the water peak was suppressed using low-power gated irradiation during the relaxation delay and during the mixing time in the NOESY spectra.

Molecular Dynamics. Molecular dynamics simulations and energy minimizations were performed using DISCOVER and INSIGHTII (Biosym Technologies Inc., San Diego, CA) on a Silicon Graphics 4D/25 Personal Iris workstation, on a Cray X-MP/48 from the San Diego Supercomputer Center (San Diego, CA), and on a Cray Y-MP8/864 from the Center for High Performance Supercomputing in Austin, TX. A full consistent valence force field, with the parameters described in ref 16, was used to calculate the potential energy. The methodology used to perform the calculations is analogous to that described in ref 5b.

Results and Discussion

Nuclear Magnetic Resonance Spectroscopy. To study the conformational behavior of the dicyclic GnRH analogue by NMR spectroscopy, we used a $CDCl_3$/DMSO-d_6 (3:2, v/v) solvent mixture. This mixture is similar to those used in previous analyses of constrained GnRH analogs,[5,9] which contained a high percentage of nonpolar solvents that promote intramolecular hydrogen bonding, such as $CDCl_3$ or tetramethylene sulfone-d_8, and a small percentage of DMSO-d_6 to avoid peptide aggregation. For the analysis of the dicyclic analogue, the percentage of DMSO-d_6 had to be increased to 40% in order to obtain line widths consistent with monomeric behavior. We also analyzed the dicyclic analogue in H_2O/TFE-d_3 (3:1, v/v) to study its behavior in a hydrophilic solvent and test the sensitivity of its conformation to the environment (see below).

To assign the proton resonances of the dicyclic analogue, we applied the sequential assignment method[17] using 2D TOCSY, NOESY, and COSY spectra (Table II). The assignment was initiated at the N-terminal acetyl group, as the corresponding methyl resonance could be easily identified at 1.75 ppm in the one-dimensional spectrum. The sequential pathway followed to assign all the backbone protons of the molecule is illustrated in Figure 2. Although severe overlapping of Hα resonances exists in the region around 4.5 ppm, the presence of some interresidue Hβ(i)/NH(i+1) and NH(i)/NH(i+1) connectivities helped resolve ambiguities. The pathway can be closed through both the Asp^4-Dpr^{10} and the Glu^5-Lys^8 bridges that bring about the dicyclic structure of the molecule. All the side-chain resonances were assigned using through-bond and/or through-space intraresidue connectivities.

Conformational information on the dicyclic GnRH analogue was obtained from amide accessibility data, nuclear Overhauser effects (NOEs), and coupling constants. The accessibility of amide protons to the solvent was probed by measuring chemical shift temperature coefficients (Table III), which were obtained from a series of TOCSY spectra recorded between 4.6 and 41.3 °C. No major conformational changes occur within this temperature range, as judged from the linearity in the dependence of the amide proton chemical shifts on the temperature. The D-Trp^3 NH, Lys^8 NH, and Lys^8 NH$^\zeta$ are sequestered from the solvent, while the Glu^5 NH and Leu^7 NH also appear to be somewhat inaccessible to the environment. All these protons have relatively low-field chemical shifts and may participate in intramolecular hydrogen bonding.

Table II. ^{1}H Chemical Shifts for the Dicyclic GnRH analogue[a]

residue	NH	H$^\alpha$	H$^{\beta1}$	H$^{\beta2}$	others
Ac^0					CH_3 1.75
D-2Nal^1	7.93	4.51	3.00[b]	2.79[c]	H$^{\delta1}$ 7.55, H$^{\delta2}$ 7.24, H$^{\epsilon3}$ 7.74, H$^{\eta1}$H$^{\eta2}$ 7.65, H$^{\eta1}$/H$^{\delta}$ 7.36
D-*p*ClPhe^2	7.91	4.44	2.98[b]	2.73[c]	H$^{\delta}_2$ 7.08, H$^{\epsilon}_2$ 7.05
D-Trp^3	7.73	4.52	3.19[c]	3.02[b]	H$^{\delta1}$ 7.10, H$^{\epsilon3}$ 7.51, H$^{\zeta2}$ 7.22, H$^{\zeta3}$ 6.93, H$^{\eta2}$ 6.98, H$^{\epsilon1}$ 10.39
Asp^4	8.17	4.49	2.74[b]	2.63[c]	
Glu^5	8.42	4.25	2.09	2.03	H$^{\gamma1}$, 2.27, H$^{\gamma2}$ 2.19
D-Arg^6	8.30	4.00	1.88	1.66	H$^{\gamma}_2$ 1.56, H$^{\delta2}$ 3.11, NH$^{\epsilon}$ 7.48, H$^{\eta1}_2$ 7.22, H$^{\eta2}_2$ 6.65
Leu^7	8.08	4.00	1.86	1.66	H$^{\gamma}$ 1.54, H$^{\delta1}_3$ 0.84, H$^{\delta2}_3$ 0.78
Lys^8	7.57	4.39	1.82[d]		H$^{\gamma}_2$ 1.44, H$^{\delta}_2$ 1.54, H$^{\epsilon}$ 3.21, H$^{\zeta2}$ 2.94, NH$^{\zeta}$ 7.51
Pro^9		4.24	2.05	1.82	H$^{\gamma1}$ 2.05, H$^{\gamma2}$ 1.82, H$^{\delta1}$ 3.78, H$^{\delta2}$ 3.51
Dpr^{10}	8.11	4.51	3.84	3.04	NH$^{\gamma}$ 7.42
NH$_2$					NH$_2^1$ 7.35, NH$_2^2$ 6.92

[a] Obtained in $CDCl_3$/DMSO-d_6 (3:2, v/v) at 23 °C. Chemical shifts were referenced to the residual DMSO solvent signal (at 2.49 ppm); uncertainty ±0.02 ppm. [b] *Pro-R*. [c] *Pro-S*. [d] H$^\beta$ magnetically equivalent.

A series of NOESY spectra with mixing times of 0.075, 0.100, 0.150, and 0.200 s were acquired to measure interproton distances (Table IV) assuming a linear dependence between NOE volume integrals and the inverse sixth power of the distance between the interacting protons. Averaged volumes calculated from the D-Trp^3 H$^{\beta1}$/H$^{\beta2}$, Asp^4 H$^{\beta1}$/H$^{\beta2}$, and Lys^8 H$^{\epsilon1}$/H$^{\epsilon2}$ interactions were used as a reference, assuming that the distance between methylene protons is 1.75 Å. The measurements obtained for the distances between aromatic protons and between Pro^9 H$^\delta$ protons, which are fixed, can be used to assess the accuracy of the data. The interproton distances that could be measured most reliably were used in the restrained molecular dynamics simulations described below, and the other distances were used to check the consistency of the conformational model developed from these calculations. The error margins of the restraints were estimated according to the intrinsic error associated with the technique[18] and from the scattering observed in the data obtained at different mixing times. Measurement of ^{13}C longitudinal relaxation times (data not shown) indicated that errors due to different mobilities in different parts of the molecule should fall within the estimated error boundaries.[19]

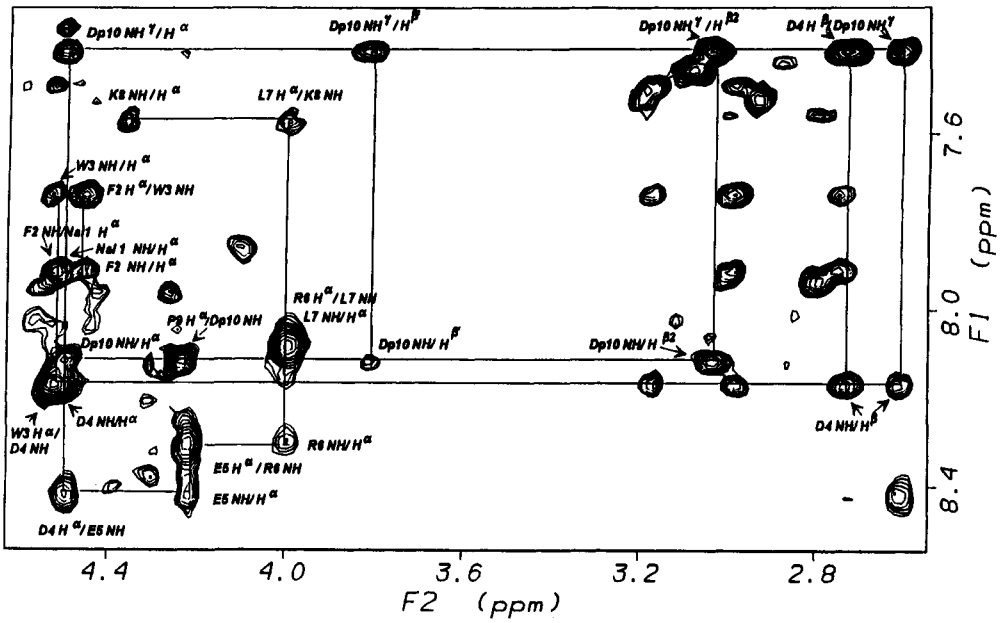

Figure 2. Contour map of the region connecting amide and H_α protons in a 500-MHz ^1H phase-sensitive NOESY spectrum of the dicyclic GnRH analogue. The pathway followed to sequentially assign the backbone protons of the molecule is illustrated. Cross-peaks within a residue are also observed in the TOCSY spectrum.

Table III. Amide Temperature Coefficients of the Dicyclic GnRH Analogue[a]

amide proton	$\Delta\delta/\Delta T$	amide proton	$\Delta\delta/\Delta T$
D-2Nal[1] NH	4.3	Lys[8] NH	1.2
D-pClPhe[2] NH	4.4	Lys[8] NH$^\zeta$	2.0
D-Trp[3] NH	1.0	Dpr[10] NH	7.1
Asp[4] NH	6.1	Dpr[10] NH$^\gamma$	4.3
Glu[5] NH	3.3	NH_2^1	5.9
D-Arg[6] NH	5.0	NH_2^2	5.0
Leu[7] NH	3.2		

[a] $\Delta\delta/\Delta T$ (ppb/K) in $CDCl_3$/DMSO-d_6 (3:2 v/v).

Most NOEs described in Table IV correspond to intraresidue or sequential connectivities. Three of these interactions, D-pClPhe[2] NH/D-Trp[3] NH, D-Trp[3] NH/Asp[4] NH, and Leu[7] NH/Lys[8] NH (Figure 3a), indicate proximity between consecutive amide protons, which in small peptides such as the dicyclic GnRH analogue are suggestive of turn conformations. Only one medium-range NOE, between Asp[4] H^α and Pro[9] H^α (Figure 3b), could be observed. This NOE could not be quantitated due to its proximity to the diagonal, but the distance between these two protons can be estimated to be less than 4 Å given the sensitivity of the NOESY data. The scarcity of medium-range interactions hinders the conformational analysis of the dicyclic analogue, but, as will be seen below, the measured interproton distances, together with the amide accessibility data and the constraints imposed by the covalent structure of the molecule, are sufficient to define the conformation of the dicyclic region of the analogue and to analyze the behavior of the linear tail (residues 1–3).

The measurement of coupling constants was hindered by broad lines and signal overlapping, but several $^3J_{HN\alpha}$ couplings could be obtained (Table V). These data were used to estimate ϕ angles[20] for the corresponding amino acid residues and to assess the consistency of our restrained molecular dynamics analysis. In addition, $^3J_{\alpha\beta}$ coupling constants for Asp[4] and for the aromatic residues (Table V) were used in stereospecific assignment of H^β protons and determination of preferred side-chain rotameric states.[21] In D-2Nal[1], the $^3J_{\alpha\beta 2}$ coupling constant is large and $H^{\beta 2}$ is closer to D-2Nal[1] NH than is $H^{\beta 1}$, indicating that the preferred rotameric state has $\chi_1 = 60°$. The same conclusion can be drawn for D-pClPhe[2], while the two small $^3J_{\alpha\beta}$ coupling constants in D-Trp[3] show that the $\chi_1 = -60°$ rotamer is preferred in this residue. The coupling constants in Asp[4], in combination with the molecular dynamics simulations described below, indicate that $\chi_1 = -60°$ predominates, but $\chi_1 = 180°$ is also substantially populated. The stereospecific assignments of H^β protons resulting from this analysis are indicated in Table II.

Conformational Interpretation. The major form of the dicyclic GnRH analogue in $CDCl_3$/DMSO-d_6 (3:2, v/v) has all the peptide bonds in the trans conformation, as indicated by the sequential H^α_i/NH_{i+1} NOEs and by NOEs between Ac[0] CH_3 and D-2Nal[1] NH, Lys[8] H^α and Pro[9] H^δs, Glu[5] H^γs and Lys[8] NH^ζ, and Asp[4] H^βs and Dpr[10] NH^γ. Analysis of interproton distances and NH temperature coefficients in the dicyclic part of the molecule shows that residues 5–8 adopt a short β-hairpin-like structure that includes a Type II′ β turn around residues 6–7 and transannular hydrogen bonds between Glu[5] NH and Lys[8] CO and between Lys[8] NH and Glu[5] CO (Figure 4). The presence of the β turn closed by the latter hydrogen bond is supported by the short D-Arg[6] H^α/Leu[7] NH and Leu[7] NH/Lys[8] NH distances, the long Leu[7] H^α/Lys[8] NH distance, and the low-temperature coefficient of the Lys[8] NH. Model building, together with the relatively low accessibility of Glu[5] NH and the Asp[4] H^α/Pro[9] H^α NOE, support the proposal of the β-hairpin structure including a Glu[5] NH/Lys[8] CO hydrogen bond. This conformation is analogous to that found previously for the parent Asp[4]-Dpr[10] analogue.[5] Indeed, the interproton distances between backbone protons in residues 4–10 of the dicyclic analogue are in excellent agreement with those measured for the Asp[4]-Dpr[10] analogue, indicating that the 5–8 bridge causes minimal distorsion of the conformation in the cyclic part of the parent monocyclic analogue. The similarity in the two analogues includes the interproton distances in the Asp[4]-Dpr[10] bridge, which appears to have some flexibility in the dicyclic analogue as was observed in the Asp[4]-Dpr[10] analogue.[5] The Glu[5]-Lys[8] bridge might also

Table IV. Interproton Distances Measured by NMR for the Dicyclic GnRH Analogue[a]

interproton distance	measured	limits	interproton distance	measured	limits
		Fixed Distances			
W3 Hβ1/Hβ2[b]	1.73	1.75	P9 Hδ1/Hδ2	1.83	1.79
D4 Hβ1/Hβ2[b]	1.75	1.75	W3 NHε1/Hζ2	2.86	2.83
K8 Hε1/Hε2[b]	1.78	1.75	W3 NHε3/Hζ3	2.52	2.83
L7 Hβ1/Hβ2	1.85	1.75	Na1 Hδ2/Hε2	2.78	2.43
Dp10 Hβ1/Hβ2	2.00	1.75			
		Conformationally Dependent Distances			
Ac CH_3/Na1 NH	3.0		D4 Hβ1/Dp10 NHγ	2.7	
Na1 NH/Hα	2.5	2.3–2.8	D4 Hβ2/Dp10 NHγ	2.6	
Na1 NH/Hβ1	3.2		D4 Hα/E5 NH	2.7	2.4–3.0
Na1 NH/Hβ2	2.6		D4 Hβ1/E5 NH	3.7	
Na1 Hα/F2 NH	2.4	2.2–2.7	E5 NH/Hα	2.7	2.4–3.0
F2 NH/Hα	2.9	2.6–3.2	E5 Hα/R6 NH	2.4	2.1–2.7
F2 NH/Hβ1	3.1		R6 NH/R6 Hα	2.9	2.6–3.2
F2 NH/Hβ2	2.7		R6 Hα/L7 NH	2.4	2.2–2.7
F2 NH/W3 NH	2.8	2.5–3.0	L7 NH/K8 NH	2.7	2.4–3.0
F2 Hα/W3 NH	2.6	2.3–2.9	L7 Hα/K8 NH	3.4	3.1–3.5
F2 Hβ2/W3 NH	4.3		K8 Hα/P9 Hδ1	2.2	1.9–2.5
W3 NH/Hα	2.9	2.6–3.2	K8 Hα/P9 Hδ2	2.4	2.1–2.7
W3 NH/Hβ1	3.5		P9 Hα/Dp10 NH	2.2	1.9–2.5
W3 NH/Hβ2	2.8		Dp10 NH/Hα	2.3	
W3 NH/D4 NH	2.7	2.4–3.0	Dp10 NH/Hβ2	2.8	
W3 Hα/D4 NH	2.2		Dp10 NH/NHγ	3.4	3.1–3.7
W3 Hβ1/D4 NH	4.0		Dp10 Hα/Hβ2	2.8	
W3 Hβ2/D4 NH	3.9		Dp10 Hα/NHγ	3.0	
D4 NH/Hβ2	3.0		Dp10 Hβ1/NHγ	2.7	
D4 Hα/Hβ2	2.7		Dp10 Hβ2/NHγ	3.4	

[a] Measured in $CDCl_3$/DMSO-d_6 (3:2, v/v) at 23 °C. All distance values in Å. Error ranges are given for the distances that were used as restraints in molecular dynamics simulations. Theoretical values, rather than error estimates, are given for distances that are fixed. Abbreviations as indicated in the legend of Figure 1. [b] Interactions used to obtain reference volumes.

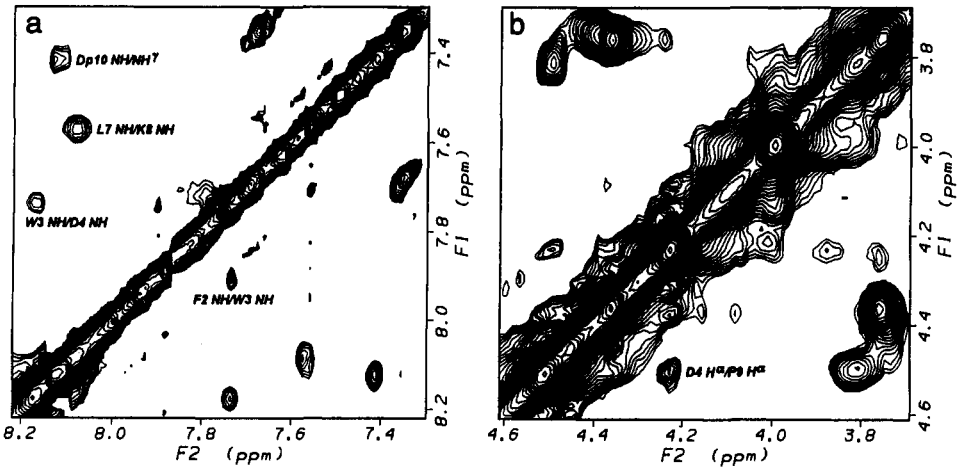

Figure 3. Contour maps corresponding to different expansions of a NOESY spectrum of the dicyclic GnRH analogue (300 ms mixing time, 23 °C): (A) amide/amide region; (B) part of the aliphatic/aliphatic region showing the only medium-range NOE observed.

Table V. Coupling Constants in the Dicyclic GnRH Analogue[a]

	D-2Nal[1]	D-*p*ClPhe[2]	D-Trp[3]	Asp[4]	Leu[7]	Dpr[10]
$^3J_{HN\alpha}$	8	8	10		8	9
$^3J_{\alpha\beta1}$	4		4	6		
$^3J_{\alpha\beta2}$	10	10	3	10		

[a] Coupling constants (Hz) measured in $CDCl_3$/DMSO-d_6 (3:2, v/v). Several couplings could not be measured due to broad lines and/or overlapping.

be expected to have some flexibility, as it is formed by several methylene groups, but the low accessibility of Lys[8] NHζ suggests that a preferred conformation exists for this bridge. As discussed below, molecular dynamics simulations indicate that Lys[8] NHζ may be hydrogen bonded to the D-Trp[3] CO.

The β-hairpin structure and the proximity of Asp[4] Hα to both Glu[5] NH and Pro[9] Hα indicate that the linear part of the dicyclic analogue, the tail formed by residues 1–3, is oriented above the plane formed by the backbone of residues 4–10, on the same side as the Glu[5]-Lys[8] bridge (Figure 4).[22] The backbone interproton distances in the tail of the dicyclic analogue are also similar to those measured for the Asp[4]-Dpr[10] analogue. However, D-*p*ClPhe[2] NH/D-Trp[3] NH and D-Trp[3] NH/Asp[4] NH NOEs are observed for the dicyclic analogue, while only the former NOE was observed for the Asp[4]-Dpr[10] analogue.[5] In addition, the D-Trp[3] NH is sequestered from the solvent, and the preferred side-chain rotamer has $\chi_1 = -60°$, which in D-amino acids is sterically unfavored.[23] This observation and the large D-Trp[3] $^3J_{HN\alpha}$ coupling constant indicate that the tail is somewhat more structured in the dicyclic analogue. The two amide/amide NOEs and the low-temperature coefficient of D-Trp[3] NH suggest that turn conformations in the tail are visited frequently, but it is unlikely that a single conformation predominates, as the D-*p*ClPhe[2] Hα/D-Trp[3] NH and D-Trp[3] Hα/Asp[4] NH distances are also short.[24] As discussed below, molecular

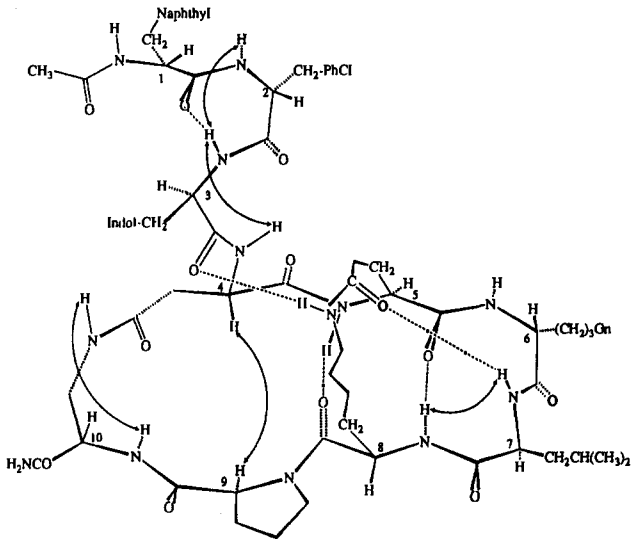

Figure 4. Conformational model for the dicyclic GnRH analogue deduced from the NMR data. Residue numbers are indicated beside the corresponding C_α carbons. Hydrogen bonds are indicated by dashed lines. Curved arrows represent amide/amide NOEs and the Asp[4] H^α/Pro[9] H^α NOE. Residues 5–8 adopt a β-hairpin conformation that includes a Type II′ β turn around residue 6–7 and is stabilized by two transannular hydrogen bonds. The tail is oriented above the ring (residues 4–10) and may interact with the 5–8 bridge, which is located on the same side of the molecule.

dynamics simulations show that the conformations visited by the tail are influenced by interactions with the Glu[5]-Lys[8] bridge, which are favored by the location of the tail and the bridge on the same side of the molecule.

To test how sensitive the conformation of the dicyclic GnRH analogue is to its environment, we also performed a series of NMR experiments in an aqueous solvent system containing H_2O/TFE-d_3 (3:1, v/v) (data not shown). The change in the hydrogen-bonding properties of the solvent results in a different hydrogen bonding pattern: in H_2O/TFE-d_3 (3:1, v/v), the only amide protons that are clearly sequestered from the solvent are Asp[4] NH and Glu[5] NH, while D-Trp[3] NH and Lys[8] NH also appear to be somewhat inaccessible. However, the backbone interproton distances in residues 5–8 are similar to those measured in $CDCl_3$/DMSO-d_6. Hence, the overall β-hairpin structure is conserved, and differences in solvent accessibility are probably produced by slight rearrangements involving librations of peptide bonds. In the tail, interproton distances and amide temperature coefficients indicate that the preferred conformations adopted in the two solvent systems are substantially different. Hence, as one would expect, the conformation in the constrained part of the molecule is rigid and well defined, while the linear part is more sensitive to the environment.

Molecular Dynamics. In order to refine the structural model of the dicyclic GnRH analogue emerging from the NMR analysis in $CDCl_3$/DMSO-d_6 (3:2, v/v) and explore further its conformational possibilities, we performed a series of molecular dynamics simulations where restraints derived from the NMR data were introduced in a progressive fashion. The process followed was analogous to that used for the Asp[4]-Dpr[10] analogue,[5] and here we will only summarize the most important results, emphasizing the features that are unique to the dicyclic analogue.

An initial conformational search *in vacuo* using high-temperature (900 K) molecular dynamics simulations, annealing simulations at 300 K, and energy minimizations, combined with torsional forcing procedures to systematically rotate all ϕ and ψ dihedral angles, yielded two fundamentally different families of conformations. These two conformational families are analogous to those found for the Asp[4]-Dpr[10] analogue *in vacuo*, without NMR restraints,[5] and differ mainly in the orientation of the tail formed by residues 1–3, which can be located below or above the 4–10 ring. As was observed for the Asp[4]-Dpr[10] analogue, when NMR restraints are introduced in simulations of the dicyclic analogue starting with tail-down structures, the tail moves above the ring, showing that only tail-up structures are compatible with the NMR data. Hence, our restrained molecular dynamics analysis was centered on the tail-up family of conformations.

The lowest energy, unrestrained tail-up structure was used to start a series of simulations incorporating NMR restraints. The 18 interproton distance restraints indicated in Table IV were introduced first, and later we added two restraints to force the transannular Glu[5] NH/Lys[8] CO and Lys[8] NH/Glu[5] CO hydrogen bonds. The lowest energy structure resulting form this simulations fitted all these NMR restraints, and its energy (141 kcal/mol) was very similar to that of the unrestrained tail-up minimum. Thus, the tail-up conformations can very easily accommodate the NMR data. During these simulations, two basically different sets of conformations were visited, differing mainly in the conformations of the tail and in the orientation of the peptide bond of the Glu[5]-Lys[8] bridge. Representative structures of these two conformational families are shown in Figure 5.

In one group of conformations, which includes the 141 kcal/mol minimum energy structure, there is a hydrogen bond between the D-Trp[3] NH and Glu[5] O^ϵ, consistent with the low-temperature coefficient of D-Trp[3] NH. The Lys[8] NH^ζ amide proton, which is also sequestered from the solvent, points toward the inside of the molecule and in some of the structures interacts with Glu[5] CO. As the side-chain rotamers in residues 1–3 did not correspond to the preferred ones observed by NMR spectroscopy, we performed simulations where we added restraints to force these rotameric states. The D-Trp[3] NH/Glu[5] CO^ϵ hydrogen bond was lost during the torsional forcing dynamics unless a restraint was added to maintain this interaction. However, structures with the preferred side-chain rotamers and the D-Trp[3] NH/Glu[5] CO^ϵ hydrogen bond could be obtained introducing such restraint, showing that the existence of this interaction is compatible with all the available NMR data. The minimum energy structure incorporating these features has an energy of 149 kcal/mol and is represented in Figure 5a.

In the other group of tail-up structures obtained with the 18 interproton distance restraints and the two transannular hydrogen bond restraints, the peptide bond in the Glu[5]-Lys[8] bridge has a different orientation, with the Lys[8] NH^ζ pointing toward the tail and interacting with D-Trp[3] CO. Glu[5] CO^ϵ is oriented toward the peptide bond in the center of the β turn and in some of the structures of this family forms a hydrogen bond with Leu[7] NH, which is partially sequestered from the solvent according to the NMR data. The simulations indicate that rather than occurring simultaneously, the Lys[8] NH^ζ/D-Trp[3] CO and Leu[7] NH/Glu[5] CO^ϵ hydrogen bonds are formed alternatively by motions of the Glu[5]-Lys[8] bridge that have a very small effect on the backbone conformation of the ring

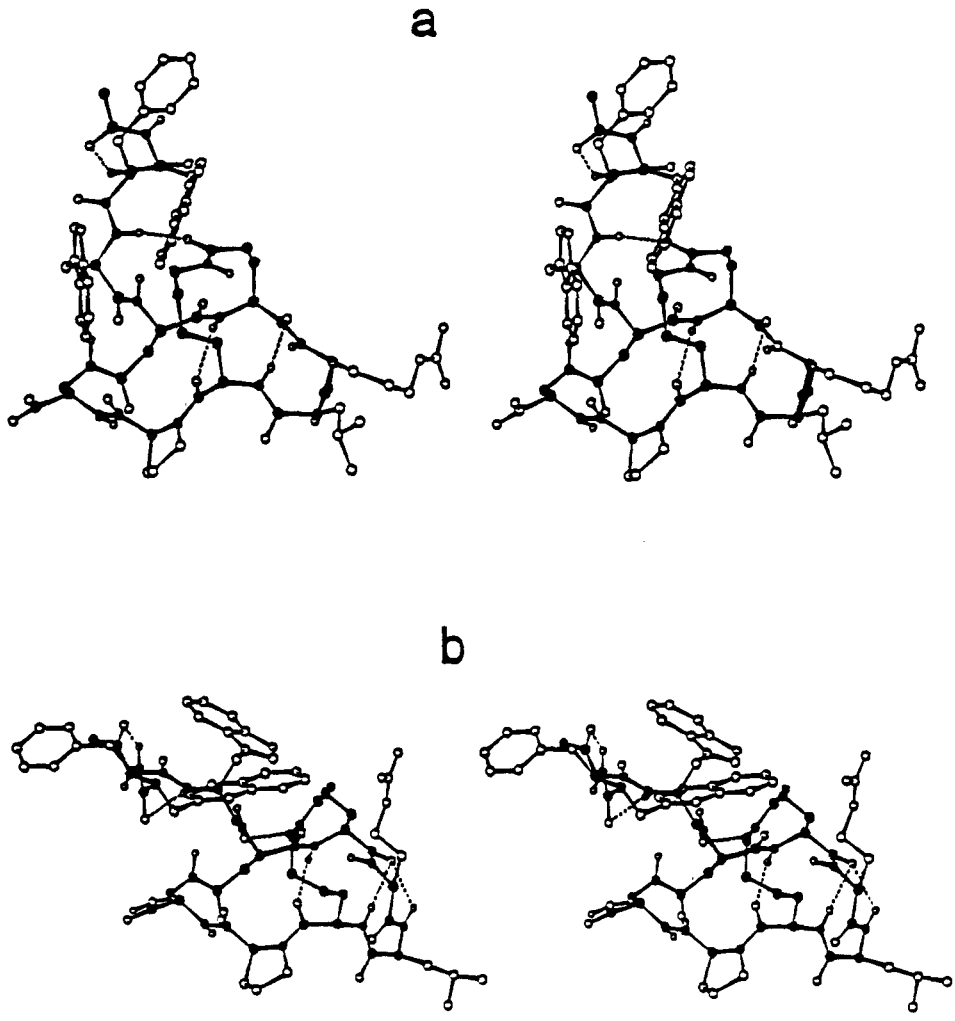

Figure 5. Stereo pairs representing selected conformations of the dicyclic GnRH analogue that fit all the NMR restraints. Only heavy atoms and amide hydrogens are shown. Dashed lines indicate hydrogen bonds. Solid circles correspond to N and C atoms in the backbone and in the Asp[4]-Dpr[10] and Glu[5]-Lys[8] bridges. (a) Minimum energy structure of the family of conformations containing the D-Trp[3] NH/Glu[5] O^{ϵ} hydrogen bond (see text); backbone dihedral angles: $\phi 1$ 85, $\psi 1$ −79, $\phi 2$ 136, $\psi 2$ −63, $\phi 3$ 154, $\psi 3$ −69, $\phi 4$ −123, $\psi 4$ 100, $\phi 5$ −144, $\psi 5$ 101, $\phi 6$ 77, $\psi 6$ −103, $\phi 7$ −81, $\psi 7$ −20, $\phi 8$ −87, $\psi 8$ 119, $\phi 9$ −84, $\psi 9$ 156, $\phi 10$ −83, $\psi 10$ 85. (b) Minimum energy structure of the family of conformations with a Lys[8] NH^{ζ}/D-Trp[3] CO hydrogen bond (see text); backbone dihedral angles: $\phi 1$ 81, $\psi 1$ −84, $\phi 2$ 91, $\psi 2$ −37, $\phi 3$ 150, $\psi 3$ 58, $\phi 4$ −97, $\psi 4$ 86, $\phi 5$ −94, $\psi 5$ 65, $\phi 6$ 73, $\psi 6$ −88, $\phi 7$ −89, $\psi 7$ −25, $\phi 8$ −81, $\psi 8$ 119, $\phi 9$ −79, $\psi 9$ 162, $\phi 10$ −83, $\psi 10$ 86.

formed by residues 4–10. The minimum energy structure in this family of conformations found during the initial simulations has an energy of 157 kcal/mol, and incorporation of the preferred side chain rotamers in residues 1–3 resulted in a slightly lower energy minimum (155 kcal/mol), which is represented in Figure 5b.

Although in all the structures obtained by restrained molecular dynamics simulation the tail formed by residues 1–3 is oriented above the ring, a variety of conformations of the tail were visited during the simulations. As predicted from the NMR data, turn conformations in the tail were visited frequently along the trajectories. A γ turn around D-*p*ClPhe[2] favored by a D-Trp[3] NH/D-2Nal[1] CO hydrogen bond was particularly persistent in the second family of structures (which lack the D-Trp[3] NH/Glu[5] CO^{ϵ} interaction), but several other tail conformations were also observed in this family. The diversity of tail conformations compatible with the NMR restraints is exemplified by the structures in Figure 5: while in the structure of Figure 5a all the residues of the tail are located above the ring, a good part of the tail in the structure of Figure 5b is pointing outward, in a more equatorial orientation. These observations confirm the conclusions drawn from the NMR analysis indicating that conformational averaging exists in the tail, despite the fact that it appears to be more structured than in the Asp[4]-Dpr[10] analogue. It is likely that the structures visited in the simulations represent only a fraction of the tail conformations that are actually visited by the dicyclic analogue in the experimental conditions used in this study.

Most energy-minimized structures of the dicyclic analogue obtained by molecular dynamics simulation including all NMR restraints have energies between 149 and 164 kcal/mol. The structures with the tail extending further from the dicyclic part of the molecule (e.g., Figure 5b) have higher energies than the more compact structures with the tail above the Glu[5]-Lys[8] bridge (e.g., Figure 5a). These higher energies are mainly due to a larger number of favorable nonbonding (van der Waals and Coulombic) interactions in the latter type of conformations. Lower energy differences (about 5 kcal/mol) were observed in molecular dynamics simulations of representative structures of the two types of conformations embedded in a bath of $CDCl_3$ molecules, due to a more favorable solvation of the more extended structures. These observations parallel our results for the Asp[4]-Dpr[10] analogue, which showed that large energy differences between structures obtained *in vacuo* (more than 25 kcal/mol) could be

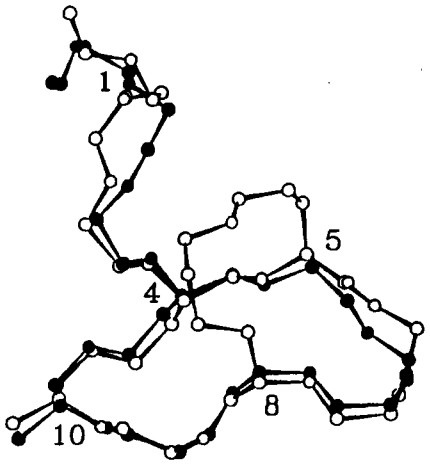

Figure 6. Superposition of the backbone atoms of the structure of the dicyclic GnRH analogue represented in Figure 5a (○) and one of the structures obtained for the parent Asp[4]-Dpr[10] analogue (●).[5] The N and C atoms of the bridges are also shown. The positions of the N-terminus and the bridged residues are indicated by numbers beside the corresponding Cα carbons. The backbone rms deviation between these two structures is 0.86 Å; the rms deviation for the backbone atoms of residues 4–10 is 0.38 Å.

ascribed to the lack of solvent in the calculations rather than to real strain energy.[5]

Our molecular dynamics results indicate that several conformations can be adopted by the dicyclic GnRH analogue which have similar energies in solution and are compatible with the NMR data. However, the conformational rearrangements in the tail and in the Asp[4]-Dpr[10] and the Glu[5]-Lys[8] bridges have small effects on the backbone conformation of the main ring, as the root mean square (rms) deviations between the backbone atoms of residues 4–10 in structures with different conformations in the tail or in the bridges are in general smaller than 1 Å. Hence, the backbone conformation of the 4–10 ring is well defined. Moreover, this conformation is very similar to that adopted by the parent Asp[4]-Dpr[10] analogue as the backbone rms deviations for residues 4–10 between structures of the two analogues are around 1 Å or smaller. The similarity between the structures of the dicyclic and the Asp[4]-Dpr[10] GnRH analogues is illustrated in Figure 6, where the backbone atoms of the structure in Figure 5a have been superimposed with the backbone of one of the structures found for the Asp[4]-Dpr[10] analogue.

Conclusion

Through conformational analysis of increasingly constrained GnRH analogues, we are developing a structural model for the biologically active conformation of GnRH. Study of a monocyclic Asp[4]-Dpr[10] GnRH analogue[5] led to a proposed conformation for residues 4–10, which consists of a β-hairpin encompassing residues 5–8 with a Type II′ β turn around residues 6–7. In this conformation, the tail formed by residues 1–3 and the side chains of residues 5 and 8 are on the same side of the molecule, which suggested new bridging possibilities to obtain more constrained, dicyclic GnRH analogues.

Introduction of a 5–8 bridge has now led to highly potent, dicyclic GnRH antagonists (Table I). This is one of the first examples where analogues of a linear peptide hormone have been constrained to such a degree with retention of high biological activity. The analysis of the dicyclic (4–10,5–8) analogue presented here shows that the 5–8 bridge does not significantly perturb the conformation of the 4–10 cycle found for the parent monocyclic antagonist. These results give strong support to the hypothesis that this conformation is essential for GnRH antagonistic activity.

Although the conformation of the 4–10 ring is well defined in our putative binding model for GnRH antagonists, a number of questions still remain about the binding mode and about the conformational requirements in the N-terminal region. Are any of the residues in the β-hairpin (residues 5–8) directly involved in the interaction with the receptor, or is this conformational feature only required to bring into proximity the N- and the C-termini? In both the Asp[4]-Dpr[10] analogue and the dicyclic analogue, the tail formed by residues 1–3 is flexible, and hence there is a smaller likelihood that the conformations visited in solution by these compounds correspond to their active conformation. However, our analysis of the dicyclic analogue shows that the orientation of the tail above the ring favors its interactions with the side chains of residues 5 and 8, in correlation with the results obtained for the Asp[4]-Dpr[10] analogue. The bridging possibilities suggested by these interactions should be extremely useful to define the active conformation in residues 1–3. Indeed, we have already synthesized a series of compounds with bridges between tail residues and residue 5 or 8, and some active compounds have been obtained.[25] We are currently analyzing the conformations adopted by these compounds to refine our model for the active conformation of GnRH.

References

(1) (a) Vickery, B. H., Nestor, J. J., Jr., Hafez, E. S. E., Eds. *LHRH and Its Analogues: Contraceptives and Therapeutic Applications*, MTP Press: Lancaster, England, 1984. (b) Karten, M.; Rivier, J. Gonadotropin-Releasing Hormone Analog Design. Structure-Function Studies Toward the Development of Agonists and Antagonists: Rationale and Perspective. *Endocr. Rev.* **1986**, *7*, 44–66.

(2) Chary, K. V. R.; Srivastava, S.; Hosur, R. V.; Boy, K. B.; Govil, G. Molecular conformation of gonadoliberin using two-dimensional NMR Spectroscopy. *Eur. J. Biochem.* **1986**, *158*, 323–332.

(3) (a) Donzel, B., Rivier, J., Goodman, M. Synthesis of a Cyclic analog of Luteinizing Hormone Releasing Factor: [Glu[4],D-Ala[6],Orn[7]]LRF. *Biopolymers* **1977**, *16*, 2587–2590. (b) Rivier, J.; Rivier, C.; Perrin, M.; Porter, J.; Vale, W. GnRH Analogs: Structure–Activity Relationships. In *LHRH Peptides as Male and Female Contraceptives*; Zatuchni, G. I., Shelton, J. D., Sciarra, J. J., Eds.; Harper & Row: Philadelphia, 1981; pp 13–23. (c) Hruby, V. J. Conformational restrictions of biologically active peptides via amino acid side chain groups. *Life Sci.* **1982**, *31*, 189–199. (d) Struthers, R. S.; Tanaka, G.; Koerber, S.; Solmajer, T.; Baniak, E. L.; Gierasch, L. M.; Vale, W.; Rivier, J.; Hagler, A. T. Design of Biologically Active, Conformationally Constrained GnRH Antagonists. *Proteins* **1990**, *8*, 295–304. Rizo, J.; Gierasch, L. M. Constrained Peptides; Models of Bioactive Peptides and Protein Substructures. *Annu. Rev. Biochem.* **1992**, *61*, 387–418.

(4) Rivier, J.; Kupryszewski, G.; Varga, J.; Porter, J.; Rivier, C.; Perrin, M.; Hagler, A.; Struthers, S.; Corrigan, A.; Vale, W. Design of Potent Cyclic Gonadotropin Releasing Hormone Antagonists. *J. Med. Chem.* **1988**, *31*, 677–682.

(5) (a) Rizo, J.; Koerber, S. C.; Bienstock, R. J., Rivier, J., Hagler, A. T., Gierasch, L. M. Conformational Analysis of a Highly Potent, Constrained Gonadotropin-Releasing Hormone Antagonist. 1. Nuclear Magnetic Resonance. *J. Am. Chem. Soc.* **1992**, *114*, 2852–2859. (b) Rizo, J.; Koerber, S. C.; Bienstock, R. J.; Rivier, J.; Hagler, A. T.; Gierasch, L. M. Conformational Analysis of a Highly Potent, Constrained Gonadotropin-Releasing Hormone Antagonist. 2. Molecular Dynamics Simulations. *J. Am. Chem. Soc.* **1992**, *114*, 2860–2871.

(6) Rivier, J. E.; Rivier, C.; Vale, W.; Koerber, S.; Corrigan, A.; Porter, J.; Gierasch, L. M.; Hagler, A. T. Bicyclic gonadotropin releasing hormone (GnRH) antagonists. In *Peptides: Chemistry, Structure and Biology*; Rivier, J. E., Marshall, G. R., Eds.; ESCOM: Leiden, The Netherlands, 1990; pp 33–37.

(7) Struthers, R. S.; Rivier, J.; Hagler, A. T. Design of peptide analogs: Theoretical simulation of conformation, energetics and dynamics. In *Conformationally Directed Drug Design-Peptides and Nucleic Acids as Templates or Targets*; Vida, J. A., Gorden, M., Eds.; American Chemical Society: Washington, DC, 1984; pp 239–261.

(8) Struthers, R. S.; Rivier, J.; Hagler, A. Molecular dynamics and minimum energy conformations of GnRH and Analogs: A methodology for computer-aided drug design. *Ann. N. Y. Acad. Sci.* **1985**, *439*, 81–96.
(9) Baniak, E. L., II; Rivier, J. E.; Struthers, R. S.; Hagler, A. T.; Gierasch, L. M. Nuclear Magnetic Resonance Analysis and Conformational Characterization of a Cyclic Decapeptide Antagonist of Gonadotropin-Releasing Hormone. *Biochemistry* **1987**, *26*, 2642–2656.
(10) Rivier, J.; Porter, J.; Rivier, C.; Perrin, M.; Corrigan, A.; Hook, W. A.; Siraganian, R. P.; Vale, W. New effective gonadotropin releasing hormone antagonists with minimal potency for histamine release in vitro. *J. Med. Chem.* **1986**, *29*, 1846–1851.
(11) Felix, A. M.; Wang, C. T.; Heimer, E.; Fournier, A. Applications of BOP reagent in solid phase synthesis. II. Solid phase side-chain to side-chain cyclizations using BOP reagent. *Int. J. Pept. Protein Res.* **1988**, *31*, 231–238.
(12) Davis, D. G.; Bax, A. Assignment of Complex ^{1}H NMR Spectra via Two-Dimensional Homonuclear Hartmann-Hahn Spectroscopy. *J. Am. Chem. Soc.* **1985**, *107*, 2820–2821.
(13) (a) Aue, W. P.; Bartholdi, E.; Ernst, R. R. Two-dimensional spectroscopy. Application to nuclear magnetic resonance. *J. Chem. Phys.* **1976**, *64*, 2229–2246. (b) Bax, A. *Two-Dimensional Nuclear Magnetic Resonance in Liquids*; Reidel: Boston, 1982. (c) Nagayama, K.; Kumar, A.; Wüthrich, K.; Ernst, R. R. Experimental techniques of two-dimensional correlated spectroscopy. *J. Mag. Reson.* **1980**, *40*, 321–334.
(14) (a) Jeener, J.; Meier, B. H.; Bachmann, P.; Ernst, R. R. Investigation of exchange processes by two-dimensional NMR spectroscopy. *J. Chem. Phys.* **1979**, *71*, 4546–4553. (b) Kumar, A.; Wagner, G.; Ernst, R. R.; Wüthrich, K. Buildup Rates of the Nuclear Overhauser Effect Measured by Two-Dimensional Proton Magnetic Resonance Spectroscopy: Implications for Studies of Protein Conformation. *J. Am. Chem. Soc.* **1981**, *103*, 3654–3658. (c) Macura, S.; Huang, Y.; Suter, D.; Ernst, R. R. Two-dimensional chemical exchange and cross-relaxation spectroscopy of coupled nuclear spins. *J. Magn. Reson.* **1981**, *43*, 259–281.
(15) Nagayama, K.; Wüthrich, K.; Bachmann, P.; Ernst, R. R. Two-Dimensional J-Resolved ^{1}H n.m.r. Spectroscopy for Studies of Biological Macromolecules. *Biochem. Biophys. Res. Commun.* **1977**, *78*, 99–105.
(16) Dauber-Osguthorpe, P., Roberts, V. A., Osguthorpe, D. J., Wolf, J., Genest, M.; Hagler, A. T. Structure and Energetics of Ligand binding to Protein: Escherichia coli Dihydrofolate Reductase-Trimethoprim, A Drug-Receptor System. *Proteins* **1988**, *4*, 31–47.
(17) Wüthrich, K. *NMR of Proteins and Nucleic Acids*; John Wiley and Sons: New York, 1986.
(18) Clore, M.; Gronenborn, A. Assessment of Errors Involved in the Determination of Interproton Distance Ratios and Distances by Means of One- and Two-Dimensional NOE Measurements. *J. Magn. Reson.* **1985**, *61*, 158–164.
(19) Additional details on the methodology used are discussed in ref 5.
(20) (a) Bystrov, V. F. Spin–spin coupling and the conformational states of peptide systems. *Prog. Nucl. Magn. Reson. Spectroscop.* **1976**, *10*, 41–82. Karplus, M. Contact electron-spin coupling of nuclear magnetic moments. *J. Chem. Phys.* **1959**, *30*, 11–15.
(21) Wagner, G.; Braun, W.; Havel, T. F.; Schaumann, T.; Go, N.; Wuthrich, K. Protein Structures in Solution by Nuclear Magnetic Resonance and Distance Geometry The Polypeptide Fold of the Basic Pancreatic Trypsin Inhibitor Determined using Two Different Algorithms, DISGEO and DISMAN. *J. Mol. Biol.* **1987**, *196*, 611–639.
(22) The same conclusion was drawn for the Asp^4-Dpr^{10} analogue in ref 5, where a detailed discussion on how these NOEs determine the orientation of the tail can be found.
(23) Ramachandran, G. N.; Sasisekharan, V. Conformation of Polypeptides and Proteins. *Adv. Protein Chem.* **1968**, *23*, 283–435.
(24) Note that the NH_{i+2}/NH_{i+3} distance in β turns is about 2.5 Å, but the $H^{\alpha}_{i+2}/NH_{i+3}$ distance is about 3.3 Å; in general, the only backbone conformations that can bring the H^{α} and the amide protons of a residue close at the same time to the next amide proton in the sequence correspond to energetically unfavored regions of the Ramachandran map (see ref 17).
(25) Rivier, J. E.; Gierasch, L. M.; Rizo, J.; Koerber, S. C.; Hagler, A. T.; Corrigan, A.; Vale, W.; Rivier, C. Probing the GnRH receptor with linear and cyclic analogs. In *Second Japan Symposium on Peptide Chemistry*; Shizuoka: Japan, 1993; in press.